Influence of Transbilayer Area Asymmetry on the Morphology of Large Unilamellar Vesicles

B. L.-S. Mui,* H.-G. Döbereiner,‡§ T. D. Madden,¶ and P. R. Cullis*

Departments of Biochemistry* and Pharmacology and Therapeutics,¶ University of British Columbia, Vancouver, British Columbia, V6T 1Z3 Canada; Department of Physics,‡ Simon Fraser University, Burnaby, British Columbia, V5A 1S6 Canada; and Max-Planck-Institut für Kolloid- und Grenzflächenforschung,§ 14513 Teltow-Seehof, Germany

ABSTRACT The morphological consequences of differences in the monolayer surface areas of large unilamellar vesicles (LUVs) have been examined employing cryoelectron microscopy techniques. Surface area was varied by inducing net transbilayer transport of dioleoylphosphatidylglycerol (DOPG) in dioleoylphosphatidylcholine (DOPC):DOPG (9:1, mol:mol) LUVs in response to transmembrane pH gradients. It is shown that when DOPG is transported from the inner to the outer monolayer, initially invaginated LUVs are transformed to long narrow tubular structures, or spherical structures with one or more protrusions. Tubular structures are also seen in response to outward DOPG transport in DOPC:DOPG:Chol (6:1:3, mol:mol:mol) LUV systems, and when lyso-PC is allowed to partition into the exterior monolayer of DOPC:DOPG (9:1, mol:mol) LUVs in the absence of DOPG transport. Conversely, when the inner monolayer area is expanded by the transport of DOPG from the outer monolayer to the inner monolayer of non-invaginated LUVs, a reversion to invaginated structures is observed. The morphological changes are well described by an elastic bending theory of the bilayer. Identification of the difference in relaxed monolayer areas and of the volume-to-area ratio of the LUVs as the shape-determining factors allows a quantitative classification of the observed morphologies. The morphology seen in LUVs supports the possibility that factors leading to differences in monolayer surface areas could play important roles in intracellular membrane transport processes.

INTRODUCTION

Differences between the surface areas of the two monolayers comprising a bilayer membrane can have dramatic effects on membrane morphology. This applies to biological membranes as well as lipid vesicle systems. In the case of the erythrocyte membrane, e.g., the external addition of amphipathic compounds to increase the area of the outer monolayer results in a transition from discocytic to echinocytic morphology (Sheetz and Singer, 1974). Alternatively, for giant lipid vesicles (~10 μm diameter), a larger inner monolayer surface area in comparison with the outer monolayer area can result in the formation of small internalized vesicles within the giant vesicle. (Käs and Sackmann, 1991; Farge and Devaux, 1992). While in single lipid systems these small vesicles are joined to the external giant vesicle by narrow necks, in vesicles prepared from lipid mixtures fissioning off from the parent has also been reported (Döbereiner et al., 1993). As the area of the exterior monolayer increases with respect to the inner monolayer area, a variety of shapes progressing from small vesicles inside giant vesicles to discoid shapes and then to small vesicles outside the giant vesicle have been observed (Sackmann et al., 1986; Berndl et al., 1990). These morphological changes in giant vesicles are now well understood in the context of a generalized bending theory (Evans, 1980; Svetina and Žekš, 1989; Seifert et al., 1992; Miao et al., 1994). The building blocks of this theory were recognized some time ago (Canham, 1970; Helfrich, 1973, 1974; Evans, 1974). Basically the shape of a closed lipid vesicle is the one that minimizes the elastic bending energy of the constituent membrane in a manner consistent with the constraints imposed by membrane area and enclosed volume.

There are several classes of vesicle shapes, which can be considered phases in analogy to thermodynamics. Transitions between these different phases can be induced by controlling system parameters such as area or volume (Käs and Sackmann, 1991; Berndl et al., 1990). Shapes were classified (Deuling and Helfrich, 1976) and phase diagrams obtained for two different models. The spontaneous curvature model (Miao et al., 1991; Seifert et al., 1991) recognizes the possibility of a local spontaneous curvature of the membrane caused by transbilayer lipid asymmetry or different adjacent fluids, whereas the bilayer-coupling model (Svetina and Žekš, 1989; Berndl et al., 1990; Seifert et al., 1991) focuses on the global asymmetry, which is induced by a small difference in the monolayer areas of the closed vesicle membrane. (For non-technical reviews see Lipowsky, 1991, and Wortis et al., 1993.) These two viewpoints have been subsumed in the area-differential-elasticity model, and the consequences have now been explored both theoretically (Seifert et al., 1992; Heinrich et al., 1993; Miao et al., 1994) and experimentally (Döbereiner, 1995) The aforementioned theories all assume lateral homogeneity in the membrane. However, in general there is a coupling of local composition to morphology, which results in lateral inhomogeneity (Gebhardt et al., 1977; Markin, 1981). Recently the consequences of this coupling for shapes and

Received for publication 17 January 1995 and in final form 5 June 1995.

Address reprint requests to Dr. Barbara Mui, Department of Biochemistry, Inex Pharmaceuticals, 1779 W. 75th Ave., Vancouver, B.C., V6P 6P2 Canada. Tel.: 604-264-9954; Fax: 604-264-9959; E-mail: bmui@inexpharm.com.

0006-3495/95/09/930/12 $2.00

shape transitions of vesicles have been explored for binary mixtures. (Jülicher and Lipowsky, 1993; Seifert, 1993; Döbereiner et al., 1993).

Investigations of vesicle morphology have been mainly limited to giant vesicles. In the present work we have extended these studies to large unilamellar vesicles (LUVs). It is shown that bending energies appear to be the shape-determining factors in these systems as well, and the results presented here are discussed within the framework of membrane elasticity.

Previous reports from this laboratory have detailed an ability to generate asymmetric transbilayer distributions of lipids such as phosphatidylglycerol (PG) and phosphatidic acid (PA) in mixtures with phosphatidylcholine (PC) in response to transmembrane pH gradients (Hope et al., 1989; Redelmeier et al., 1990; Eastman et al., 1991). Lipid translocation occurs through transport of the neutral (protonated) forms of PG or PA, and can result in the translocation of as much as 10% of the lipid in one monolayer across the membrane. Given that there is no evidence of any compensatory movement of PC in response to such transport (Hope et al., 1989), large changes in morphology would be expected. In this work we examine the morphological consequences of transbilayer transport of dioleoylphosphatidylglycerol (DOPG) in dioleoylphosphatidylcholine (DOPC): DOPG (9:1 mol ratio) LUVs employing cryoelectron microscopy. It is shown that a progression of morphologies eventually leading to the formation of long tubules is observed as DOPG is transported to the outer monolayer. Alternatively, when PG is transported from the outer monolayer to the inner monolayer, the reverse behavior leading to invaginated vesicles is observed. These studies establish LUV systems as useful models for examining the morphological consequences of transbilayer area differences.

MATERIALS AND METHODS

DOPC, monooleoyl PC, and DOPG were obtained from Avanti Polar Lipids, Inc. (Alabaster, AL). [^{3}H]-DPPC was obtained from Amersham Corp. (Arlington Heights, IL). Cholesterol (standard for chromatography), 2-(*p*-toluidinyl)naphthalene-6-sulfonic acid (TNS), and all buffers were supplied by Sigma Chemical Co. (St. Louis, MO). Gold 700 mesh bare electron microscopy (EM) grids were obtained from Marivac Ltd. (Halifax, Nova Scotia, Canada).

Preparation of lipid vesicles

Dry lipid mixtures were prepared by lyophilization of lipids dissolved in benzene:methanol (95:5 vol/vol) under high vacuum (≤60 mm Hg) for a minimum of 4 h. Multilamellar vesicles (MLVs) (25–50 mM lipid) were prepared by hydration of the dry lipid in an 530 mOsm/kg buffer composed of either 300 mM citrate, pH 4.0, or 300 mM HEPES, 40 mM Na_2SO_4, pH 7.5 and the dispersion was freeze-thawed five times employing liquid nitrogen and warm water cycles (50°C) to promote equilibrium transmembrane distributions of solutes (Mayer et al., 1985). LUVs were then prepared by extruding the frozen and thawed MLVs 10 times through two stacked 100 nm pore size polycarbonate filters (Nuclepore Corp., Pleasanton, CA) using an Extruder (Lipex Biomembranes, Inc., Vancouver, B.C.) as described previously (Hope et al., 1985).

Generation of DOPG asymmetry

LUVs containing DOPC and DOPG (9:1, mol:mol) and radiolabeled with 2 μCi [^{3}H]-DPPC per mM lipid were prepared in 300 mM citrate, pH 4.0 and passed down a Sephadex G-25 column pre-equilibrated with 150 mM Na_2SO_4, 1 mM citrate, pH 4.0 (330 mOsm/kg). The lipid concentration was then either adjusted to 10 mM if the sample was used for lipid asymmetry measurements or was adjusted to 20 mM if used for cryoelectron microscopy studies. To induce a net movement of DOPG to the outer monolayer, the vesicles (1 ml) were diluted with 0.4 ml of a buffer (pH 7.5) containing 300 mM HEPES and 40 mM Na_2SO_4 (530 mOsm/kg), and a 0.2 ml aliquot was incubated for various times at 60°C. DOPG transport to the outer monolayer was stopped by plunging the test tube into an ice-water mixture and rapidly swirling the contents. The sample was then stored on ice. To induce a net transport of DOPG from the outer monolayer to the inner monolayer, a pH gradient where the interior is basic with respect to the external medium is required. Vesicles were therefore prepared in 300 mM HEPES, 40 mM Na_2SO_4, pH 7.5 (530 mOsm/kg) and passed down a Sephadex G-25 column pre-equilibrated with 150 mM Na_2SO_4, 1 mM HEPES, pH 7.5 (330 mOsm/kg). A pH gradient, interior basic, was generated by diluting the vesicles with a 300 mM citrate, pH 4.0 buffer (530 mOsm/kg).

Detection of asymmetry using TNS

Transbilayer distributions of DOPG were detected using the TNS assay described by Eastman et al. (1991). TNS is a fluorescent lipophilic anion that exhibits enhanced fluorescence when associated with a lipid bilayer. The presence of a negatively charged lipid such as PG will decrease TNS absorption to the membrane, resulting in a decrease in fluorescence. To perform this assay, a 0.2 ml lipid sample was first diluted with 0.5 ml of 100 mM ammonium acetate, 100 mM citrate, pH 6.0, and 0.2 ml aliquots of this dispersion were diluted into 3 ml of 3 mM TNS, 5 mM ammonium acetate, 5 mM HEPES, pH 7. The fluorescence was measured using a Perkin-Elmer (Norwalk, CT) LS-50 fluorometer at an excitation wavelength of 321 nm (bandwidth 2.5 nm) and emission wavelength of 445 nm (bandwidth 5 nm). Standard curves were constructed for DOPC and DOPC:Chol (6:3, mol:mol) vesicles containing various amounts of DOPG.

Cryoelectron microscopy

A drop of the liposomal suspension was placed on a bare 700 mesh gold EM grid held by tweezers mounted on a spring-loaded plunger. After removing excess sample by blotting the grid with filter paper, the sample was vitrified by plunging the grid into liquid propane cooled to −187°C. Blotting and vitrification was performed rapidly (≤2 s) to minimize evaporation of water from the sample. The grid was then transferred to a Gatan 126 cold stage at liquid nitrogen temperatures using a Reichart Jung Universal Cryo-Fixation system, and the sample was visualized using a Zeiss EM 10C STEM (Carl Zeiss, Oberkochen, Germany). As induced DOPG asymmetry was found to be stable for 20 h at 4°C, samples were kept on ice (maximum 7 h) before use. Lipid asymmetry was checked before and after cryoelectron microscopy.

Analytical procedures

Phospholipid concentrations were determined by phosphate assay (Fiske and Subbarow, 1925) and radiolabels quantified by liquid scintillation counting on a Beckman (Fullerton, CA) LS3801 instrument. Solution osmolarities were determined from freezing point depression using an Advanced Digimatic 3C2 osmometer (Precision Systems, Inc., Natick, MA).

RESULTS

The first series of experiments was performed to characterize the morphological changes observed on translocating

DOPG from the inner to the outer monolayer of 100 nm diameter DOPC:DOPG (9:1, mol:mol) LUVs. Previous studies with DOPC:DOPG (9:1, mol:mol) LUVs have shown that DOPG is transported from the outer to the inner monolayer when a pH gradient, interior basic (pH_o = 4.0, pH_i = 9.0), is applied across the LUV membrane (Redelmeier et al., 1990). This indicates that to transport DOPG in the reverse direction from the inner to the outer monolayer at equivalent rates, a pH gradient where the interior is at pH 4.0 and the exterior is basic should be utilized. An interior pH of 4.0 and an exterior pH of 7.5 were employed. The time course of DOPG translocation in response to ΔpH at 60°C was determined employing the TNS assay. The results are shown in Fig. 1, which illustrates that for both DOPC:DOPG (9:1) and DOPC:DOPG:Chol (6:1:3) vesicles, nearly complete DOPG asymmetry can be obtained after 20 min incubation at 60°C.

Morphological changes associated with the transport of DOPG to the outer monolayer were then investigated employing cryoelectron microscopy. A first objective was to obtain an accurate representation of the morphology before induction of lipid asymmetry. In this regard, whereas the transbilayer movement of DOPG in response to a pH gradient is relatively fast at 60°C, it is considerably slower at lower temperatures due to a high activation energy ($E_a \simeq 31$ kcal/mol) for DOPG transport (Redelmeier et al., 1990). It was found experimentally that no detectable translocation of DOPG from the inner to the outer monolayer occurred in DOPC:DOPG (9:1, mol:mol) LUVs with a pH gradient (pH_i = 4.0, pH_o = 7.5) during a 2 h incubation at 4°C. The morphology of LUVs that are not exposed to higher temperatures should therefore provide an accurate depiction of the initial vesicle shapes.

Representative shapes observed by cryoelectron microscopy are shown in Fig. 2 *A*. The most notable feature is the dimpled appearance of the LUVs, which could be interpreted as vesicles within vesicles. However, closer inspection of Fig. 2 *A* suggests that these structures represent invaginated LUVs, or stomatocytes, which is clearly seen in an edge-on view (Fig. 2 *A*, *solid arrow*). Note that nearly all of the vesicles seem to be rotational symmetric bodies. The axis of symmetry is indicated in the figure by a dashed line, if the symmetry axis is approximately within the projection plane, and with a cross if it is perpendicular to it. In one vesicle (Fig. 2 *A*, *open arrow*), the symmetry axis of which is at a small angle to the projection plane, the rounded open neck of the stomatocyte is seen in a perspective view. The volume-to-area ratio of the LUVs is varying slightly as can be inferred from the different radii of the outer and inner membranes of the stomatocytes. In most of the LUVs the inner monolayers seem to be in contact at the opposing side of the stomatocyte opening (Deuling and Helfrich, 1976).

As indicated in the Introduction, the non-spherical invaginated morphology can be attributed to an excess of surface area of the inner monolayer relative to the outer monolayer. That this is indeed the case is demonstrated by translocation of DOPG to the outer monolayer, whereby the area of the inner monolayer is reduced and the invaginated structures disappear. In Fig. 2, *B* and *C*, DOPC:DOPG (9:1, mol:mol) LUVs that have been incubated at 60°C for 3 and 20 min, respectively, are shown. Translocation of DOPG to the outer monolayer results in a transformation into long tubular

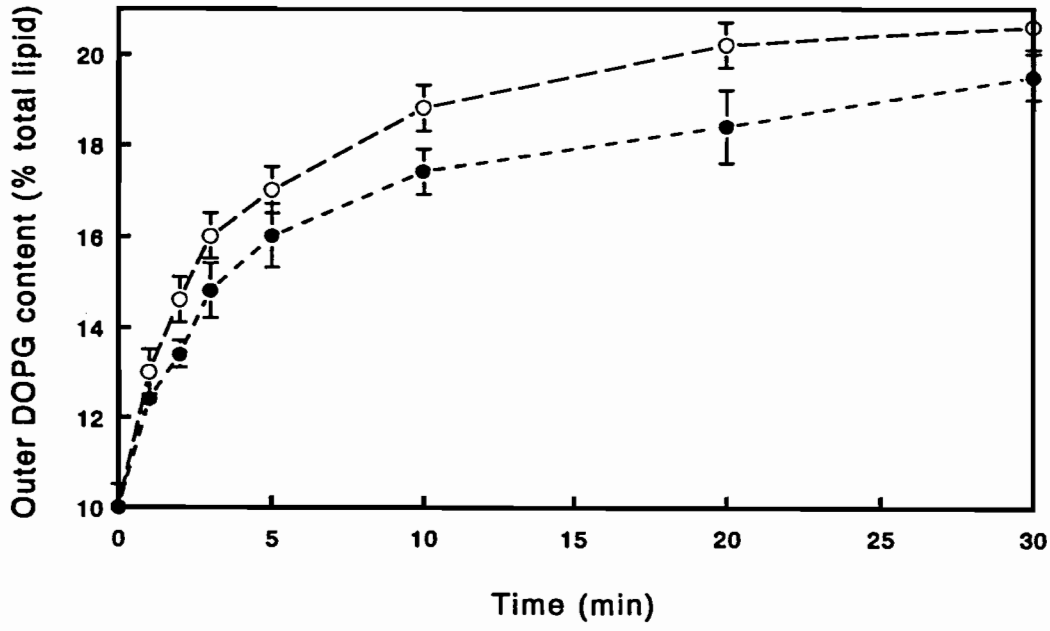

FIGURE 1 Quantitation of DOPG asymmetry induced by a pH gradient (pH_o = 7.5, pH_i = 4.0). The amount of DOPG present in the outer monolayer of DOPC (9:1, mol:mol; ○) or DOPC:DOPG:Chol (6:1:3, mol:mol:mol; ●) 100 nm diameter vesicles in the presence of the pH gradient and subsequently incubated at 60°C for various times was measured using the TNS assay defined in Materials and Methods. The outer monolayer DOPG concentration was determined from the TNS fluorescence using a standard curve constructed from DOPC or DOPC:Chol (6:3) vesicles containing 10–20 mol % DOPG.

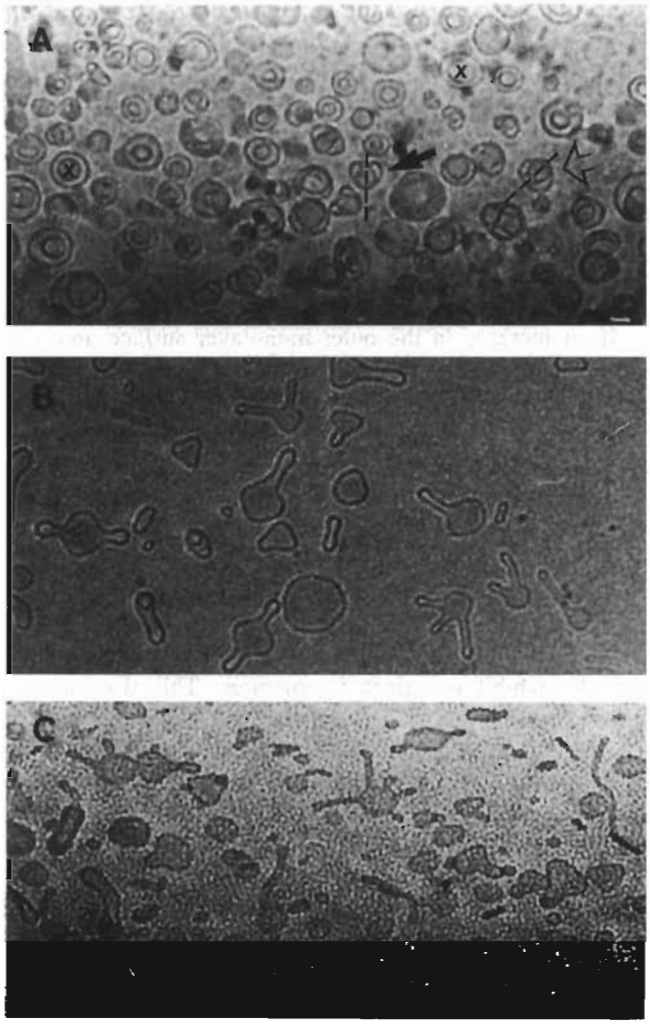

FIGURE 2 Morphological changes in DOPC:DOPG (9:1, mol:mol) vesicles generated by the transport of DOPG to the outer monolayer. Cryoelectron micrographs were taken of DOPC:DOPG (9:1) vesicles, which have been exposed to a pH gradient (pH_o = 7.5, pH_i = 4.0) and incubated at 60°C for (*A*) 0 min; (*B*) 3 min; (*C*) 20 min. The bar represents 200 nm. The axis of rotational symmetry is indicated by a dashed line, if the symmetry axis is approximately within the projection plane, and with a cross, if it is perpendicular to it.

shapes as well as vesicles exhibiting one or more projections. It would appear that more projections are seen for vesicles incubated at 60°C for 20 min. This is consistent with a larger increase in the area of the outer monolayer.

In this ensemble there is now a large percentage of non-axisymmetric bodies. However, there are also vesicles with a quite high degree of symmetry (Fig. 2 *A*), which seem to fall into distinct classes. Assuming a constant volume-to-area ratio during the shape transition, the vesicles are flattened bodies oriented within the projection plane. However, a quantitative evaluation is difficult, because no edge-on views are available. The presence of much smaller vesicles, which may have resulted from fragmentation of these tubular arms, is also evident in Fig. 2 *C*.

Similar shape changes were also observed for LUVs containing cholesterol. DOPC:DOPG:Chol (6:1:3) LUVs were prepared with an internal pH of 4.0, transferred to a medium with a pH of 7.5, and incubated at 60°C for 20 min to induce essentially complete transport of DOPG to the outer monolayer. Before induction of DOPG transport, the morphology corresponds to invaginated vesicles (Fig. 3 *A*). Note that some of the vesicles have very small internal volume, as is evident from the only slightly different outer and inner radii of these stomatocytes.

After incubation at 60°C, long tubular structures are predominant (Fig. 3 *B*). These tubular structures appear more stable than those observed with DOPC:DOPG (9:1) LUVs in that vesicle "fragments" were not observed. Note also that the thin protrusions are absent in this ensemble. This results in a higher degree of symmetry. Most notable is

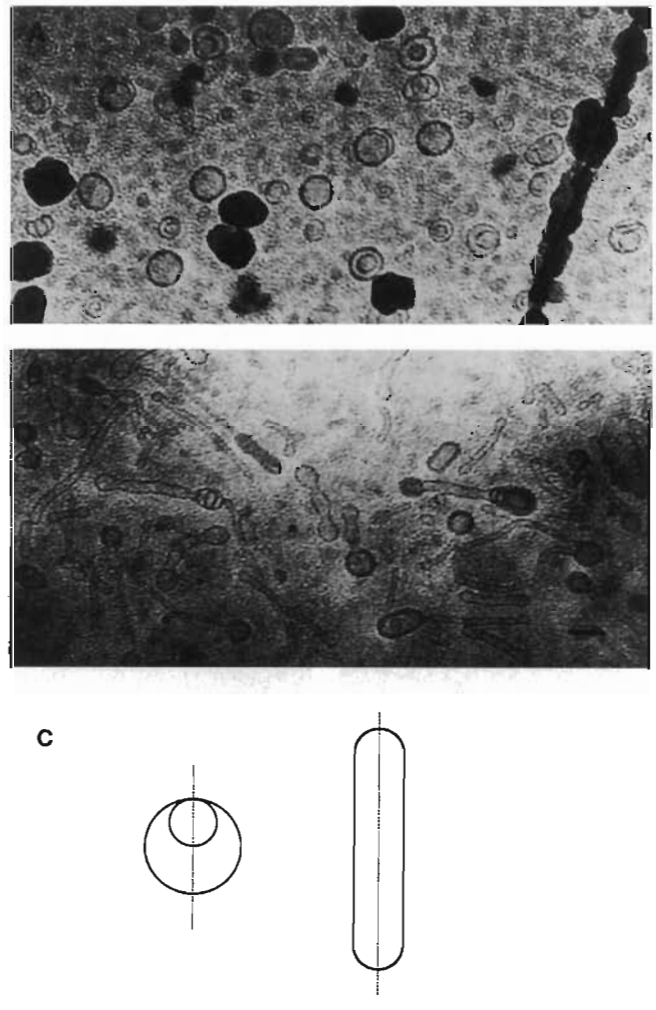

FIGURE 3 Morphological changes in 100 nm diameter DOPC:DOPG:Chol (6:1:3, mol:mol:mol) vesicles induced by the transport of DOPG to the outer monolayer. Cryoelectron micrographs were taken of DOPC:DOPG:Chol (6:1:3, mol:mol:mol) vesicles exposed to a pH gradient (pH_o = 7.5, pH_i = 4.0) before (*A*) and after (*B*) a 60°C incubation step for 15 min to generate DOPG asymmetry. The bar represents 200 nm. (*C*) Two vesicle shapes with equal area and volume (v = 0.63). The geometrical monolayer area difference Δa measures 0.45 for the stomatocyte and 1.34 for the spherocylinder relative to the sphere. (v and Δa are defined in the Discussion.) The axes of rotational symmetry are indicated by dashed lines.

the appearance of beaded tubes. We should point out that the apparent change in volume-to-area ratio of the vesicles is deceptive; in fact, for the two ensembles shown in Fig. 3, *A* and *B*, it is quite constant. This is made plausible by the two rotationally symmetric bodies shown in Fig. 3 *C*, which actually have the same volume and area. To understand this counterintuitive fact one has to realize that the volume contained in a sphere increases as the third power of its radius, whereas the volume of a tube grows only linearly with its length.

If the sequence of morphological changes in Fig. 2 is simply due to a progressive increase in exterior surface area as DOPG is transported to the outer monolayer, the external addition of lipid to the outer monolayer of the LUVs should also induce morphological changes, which are similar to those caused by the transport of DOPG. The outer monolayer area can be increased by incubating the vesicles with lysophosphatidylcholine (lyso-PC), which will readily partition into the outer monolayer. DOPC:DOPG (9:1) vesicles, in the absence of a pH gradient ($pH_i = pH_o = 4.0$), were therefore incubated with monooleoyl PC at 0–8% mol ratios of monooleoyl PC to phospholipid at constant osmolarity. Vesicles incubated with 0.5% monooleoyl PC (Fig. 4 *B*) show fewer of the invaginated structures than do vesicles that have not been exposed to monooleoyl PC (Fig. 4 *A*). In fact, most of the invaginations seem to have disappeared. The presence of higher monooleoyl PC concentrations induces further morphological changes as shown in Fig. 4, *C* and *D*. LUVs incubated with 5 and 8% monooleoyl PC depart from invaginated shapes to vesicles with tube-like projections (Fig. 4, *C* and *D*, respectively). This is consistent with a higher concentration of monooleoyl PC in the outer monolayer as required by chemical equilibrium between the lipids partitioned into the membrane and those in bulk solution. Note the appearance of vesicles with a threefold symmetry. This sequence of morphological changes is similar to that observed when PG is transported to the outer monolayer in response to a pH gradient (Fig. 2).

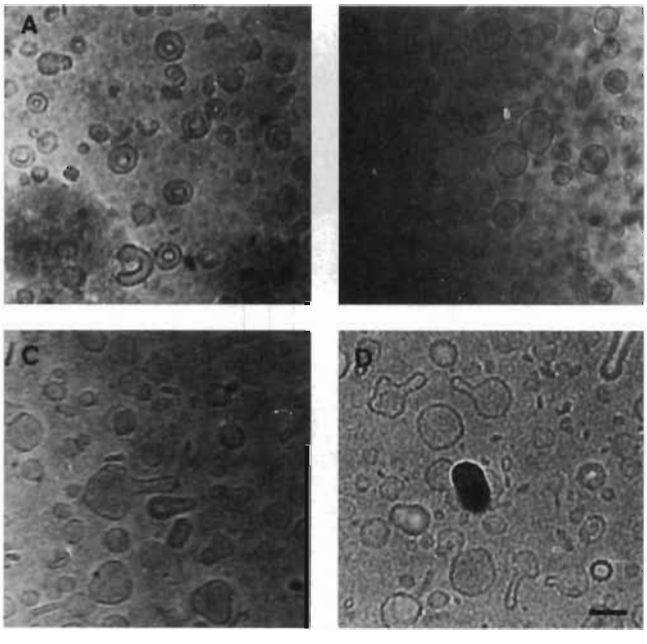

FIGURE 4 Morphological changes of DOPC:DOPG (9:1) vesicles induced by the partitioning of monooleoyl PC into the outer monolayer of the 100 nm LUVs. DOPC:DOPG (9:1) vesicles prepared in 300 mM citrate, pH 4 were incubated for 5 min at 23°C with (*A*) 0%, (*B*) 0.5%, (*C*) 5%, and (*D*) 8% mol ratios of monooleoyl PC to phospholipid in an external medium composed of 150 mM Na_2SO_4, 5 mM citrate pH 4. The bar represents 200 nm.

If an increase in the outer monolayer surface area can cause invaginated vesicles to become tubular or form tubular projections, then increasing the inner monolayer surface area should reverse this morphology and cause tubular vesicles to become invaginated. As indicated above, the area of the inner monolayer can be increased by transporting PG from the outer to the inner monolayer using a pH gradient, where the vesicle interior is basic with respect to the exterior (Hope et al., 1989; Redelmeier et al., 1990). To clearly demonstrate the effect of this inward transport of lipid, it was necessary to start with LUVs that did not already exhibit invaginated structures. This was accomplished by adding 2 mol % monooleoyl PC to the exterior of LUVs composed of DOPC:DOPG (9:1) to reduce the proportion of LUVs that exhibited invaginated morphology. These LUVs were then incubated in the presence of a pH gradient (interior basic) to transport DOPG to the inner monolayer. Fig. 5 *A* illustrates DOPC:DOPG (9:1) LUVs that have not been exposed to monooleoyl PC nor incubated at 60°C. It may be observed that in the absence of monooleoyl PC, the vesicles are predominantly invaginated. However, the vesicles become tubular after the addition of 2% monooleoyl PC to the outer monolayer (Fig. 5 *B*). As shown in Fig. 5 *C*, this morphological change can be reversed by the subsequent transport of DOPG to the inner monolayer during a 10 min incubation at 60°C. We thus see a transformation of stomatocytes to dumbbells and vice versa.

It is of interest to note that the extent of inward DOPG transport was reduced in the absence of 2% monooleoyl PC. An analysis of DOPG asymmetry induced in DOPC:DOPG (9:1, mol:mol) vesicles indicated that the maximum amount of DOPG that can be transported into the inner monolayer is 70% of the exterior DOPG, whereas complete DOPG asymmetry can be obtained for vesicles in which the outer monolayer area has been increased by a preincubation with 2% monooleoyl PC (results not shown).

DISCUSSION

Theory of shapes

It is generally accepted that lipid bilayers respond elastically to mechanical deformations (Meunier et al., 1987). These deformations include bending, and stretching or compression of the membrane. In the following, the membrane is idealized as a quasi two-dimensional sheet consisting of two monolayers. Measurements of the elastic moduli show that

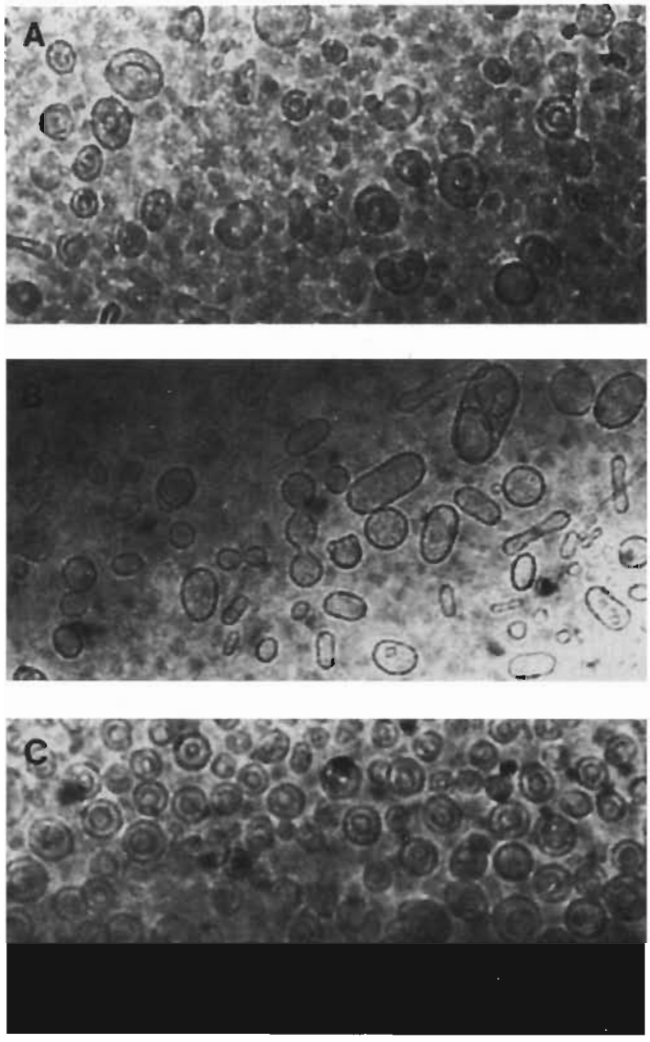

FIGURE 5 Morphological changes of DOPC:DOPG vesicles incubated with monooleoyl PC and subsequently exposed to a pH gradient (interior basic) to induce DOPG transport to the inner monolayer. DOPC:DOPG (9:1) vesicles prepared in 300 mM HEPES, 40 mM Na_2SO_4 pH 7.5 were incubated for 5 min at 23°C in the absence (*A*) and presence (*B*) of a 2% mol ratio of monooleoyl PC to phospholipid in 150 mM Na_2SO_4, 1 mM HEPES pH 7.5. Vesicles incubated with 2% monooleoyl PC were then heated to 60°C for 10 min to generate DOPG asymmetry (*C*). The bar represents 200 nm.

it is much harder to stretch a membrane than to bend it (Marsh, 1990). Elastic theories that aim to describe the morphology of membranes can thus assume to a good approximation that the overall area of the membrane is fixed. However, it turns out that the energetic contributions of the relative stretching and compression of the two monolayers, which arise when the membrane is bent, are of the same order of magnitude as the pure bending energy, which originates from splaying the molecules in the two monolayers. We have therefore two main contributions to the bending energy of a bilayer: The bending of the two monolayers at fixed bilayer area A, and the relative stretching and compression of the monolayers. This means we keep the mean area $A = (A^{out} + A^{in})/2$ fixed but allow for changes in the differential area $\Delta A = A^{out} - A^{in}$ (Fig. 6). One might object that the two leaflets are free to slide past each other and therefore no elastic deformations occur. This would indeed be the case if the edges of the membrane were unconstrained. However, in general there are no exposed hydrophobic edges and the membrane forms a closed bag of volume V. Therefore, although the bilayer can adapt locally, there will be a remaining global constraint, which is given by the overall geometry of the vesicle.

We have thus identified the geometrical quantities needed to formulate the expression for the bending energy: 1) local membrane curvature $C_i(r)$ along the two principal directions and 2) global area difference between the monolayers ΔA. It can be shown that the latter quantity is, to a good approximation, proportional to the integrated mean curvature of the vesicle

$$\Delta A = D \int dA (C_1 + C_2), \tag{1}$$

where D is the bilayer thickness. This equation makes the connection between shape and differential area explicit, and the reader is invited to verify it for the simple case of a spherical vesicle. One finds for the total energy (Miao et al., 1994)

$$E_B = \frac{\kappa}{2} \int dA (C_1 + C_2 - C_0)^2 + \frac{\bar{\kappa}}{2} \frac{\pi}{AD^2} (\Delta A - \Delta A_0)^2 \tag{2}$$

where C_0 is the spontaneous curvature of the membrane, which accounts for a possible non-flat relaxed state of the bilayer, $\Delta A_0 = A_0^{out} - A_0^{out}$ is the difference of the unstressed monolayer areas, and κ and $\bar{\kappa}$ are the local and non-local bending moduli of the membrane, respectively. In the first term, one simply integrates the local deviations in mean curvature from the relaxed state over the whole vesicle area. The second term accounts for the difference between the actual geometrical area difference and the relaxed one, which would be preferred by the monolayers. (This equilibrium differential area is proportional to the difference in the number of molecules: $\Delta A_0 = a_{lipid}^{in} N^{in} - a_{lipid}^{out} N^{out} \simeq \overline{a_{lipid}} \Delta N$.) Both terms are quadratic and correspond to a

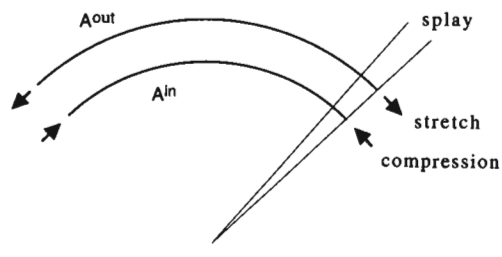

FIGURE 6 Elastic deformations. Bending the bilayer results in splaying of the molecules in the individual monolayers. In addition, when the membrane is bent at fixed mean monolayer area $A = (A^{out} + A^{in})/2$, the outer monolayer is stretched and the inner monolayer is compressed relative to each other, or vice versa.

generalization of Hooke's law for the spring to bending and differential area elasticity. The relative importance of the two terms is measured by the ratio of the two elastic moduli

$$\alpha = \frac{\bar{\kappa}}{\kappa}.$$

For $\alpha = 0$, there is no resistance to bending from differential area elasticity, and the spontaneous curvature model is recovered (Helfrich, 1973). For $\alpha = \infty$, the geometrical area difference ΔA does not deviate from the preferred area difference ΔA_0 of the monolayers. This is the essence of the bilayer-couple hypothesis put forward by Sheetz and Singer (1974) and formulated in the context of elasticity theory by Evans (1974, 1980) and Helfrich (1974). However, an estimate of α gives 1.1 for dimyristoyl PC and generally is of the order of 1 for all phospholipids (Miao et al., 1994). This estimate is corroborated by recent measurements of this quantity (Waugh et al., 1992). Both terms are therefore important and it would be wrong to think in either of the two limits. Indeed, experiments on shapes and shape transitions in giant vesicles have shown that the general model is required to account quantitatively for the observations (Döbereiner, 1995).

The shape of an individual fluid bilayer vesicle is one that minimizes the bending energy (Eq. 2) given the geometrical parameters area A and volume V, as well as the material parameters moduli ratio α, the spontaneous curvature C_0, and the equilibrium area difference ΔA_0. When these parameters are tuned externally the shape changes. Different regions of the parameter space correspond to different classes of shapes. (These classes result from the existence of multiple solutions to the shape equations, derived by minimizing Eq. 1.) At the boundary between those regions shape transitions occur, which are manifested, e.g., in a change of symmetry or another shape attribute. In Fig. 7 a cartoon of this correspondence between shape parameters and vesicle morphologies is shown.

In Fig. 5, for example, we see transitions from stomatocytes, which have no equatorial symmetry, to equatorial symmetric shapes such as ellipses or dumbbells (Seifert et al., 1991) and vice versa. Another specific shape attribute is the number of beads, and vesicles with different numbers would correspond to different classes (Miao et al., 1991). A few members of these special classes can be identified in Figs. 3 *B* and 5 *B*. What variables are relevant for an understanding of the observed shapes and shape transitions in LUVs? The parameters controlled in this experiment are the area and volume of the vesicles and the area difference between the monolayers. As we have already argued, the area can be considered fixed at constant temperature. Since the membrane is permeable to water the volume is controlled by the osmolarities of the inner and outer solutions. Any osmolarity differences would lead to large osmotic forces inducing water flow through the membrane. It is thus the permeability of the membrane to water that is responsible for the constancy of the enclosed water volume at

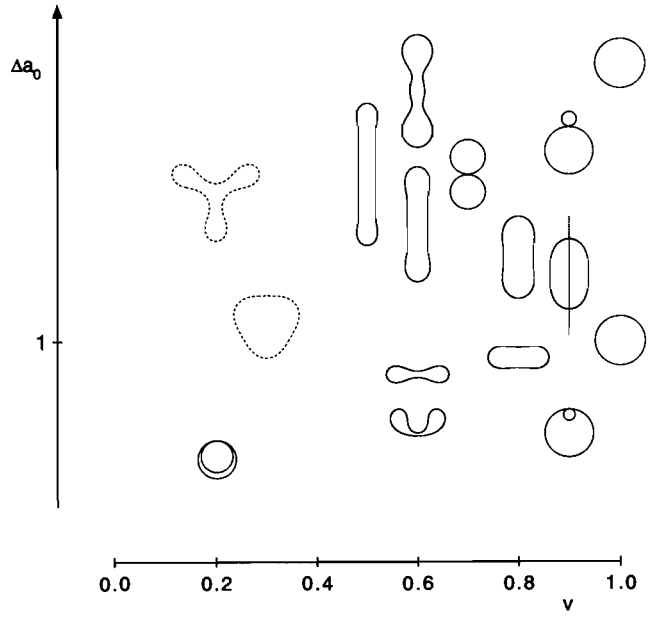

FIGURE 7 Schematic phase diagram of vesicle shapes. This phase diagram shows the shapes of lowest bending energy for given reduced volume v and equilibrium differential area $\Delta a_0 = m_0/(4\pi)$. The axes of rotational symmetry are along the vertical. The dashed contours depict non-axisymmetric shapes.

given osmolarity. The amount of osmolarity difference that can be sustained by a curved membrane depends on the curvature scale. It can be estimated by equating the change in bending energy E_B with volume V to the osmotic pressure (Seifert et al., 1991) $\partial E_B/\partial V \simeq 8\pi\kappa/V = RT\,\Delta n$, where R is the gas constant, T the temperature, and Δn the molarity difference. With $\kappa = 10^{-19}$ J and $V = 4\pi/3\ (50\ nm)^3$, one finds at room temperature $\Delta n \simeq 2$ mM/l. With the osmolarities employed in this study we can thus neglect any cross-coupling of bending with osmotic forces. The volume-to-area ratio is fully controllable for LUVs and does not adjust via shape changes. (We realize, however, that the scale enters with the third power and smaller membrane structures could sustain large osmotic gradients without being significantly stretched.) During shape changes induced by controlling the equilibrium differential area ΔA_0, the area A and volume V of the LUVs can thus be considered constant.

It turns out that area and volume do not enter separately in determining the shape. It is the volume-to-area ratio that is important, and we define the dimensionless quantity

$$v = \frac{V}{(4\pi/3)R_A^3}, \qquad (3)$$

where $R_A = (A/4\pi)^{1/2}$ is the area-equivalent radius. This reduced volume v is scaled so that a sphere is characterized by unity, the maximum value of volume-to-area ratio possible for any geometrical object. Deflated vesicles have values <1, and 0 would correspond to an empty membrane bag without any aqueous content. The reduced volume v

represents a convenient measure of the enclosed volume of a vesicle, stripped of the size information.

Apart from this purely geometrical quantity one needs a parameter that describes the overall tendency of the membrane to curve. It is given by a dimensionless combination of the spontaneous curvature and the area difference.

$$\bar{m}_0 = 4\pi\Delta a_0 + \frac{2}{\alpha} c_0, \tag{4}$$

where $\Delta a_0 = \Delta A_0/8\ \pi D R_A$ and $c_0 = C_0 R_A$ are scaled quantities. Again this scaling singles out the sphere. A spherical vesicle with radius R_A, a scaled spontaneous curvature $c_0 = 1$, and an scaled area difference $\Delta a_0 = 1$, is in a totally relaxed state with energy zero. It would have no differential area stresses and no bending stresses in its membrane. It is clear that this is a rather special situation. In general, a vesicle will be in a stressed state, its morphology being determined by the most relaxed shape possible consistent with constraints imposed. The effective spontaneous curvature $\bar{m}_0$ is thus reflecting the different sources of membrane curvature. A large area difference $\Delta a_0 > 1$ tends to curve the membrane outward, whereas a smaller or negative value would lead to invaginated shapes. Likewise, a spontaneous curvature c_0 other than 1 would favor outward or inward curved shapes with respect to the sphere. (A flat membrane sheet would be stable for $c_0 = 0$.) Of course it is really the combination of both that determines the shape, the relative contributions being fixed by the ratio of the elastic moduli α. This is intuitively clear, because the shape changes to adopt the minimal energy configuration and the balance is shifted according to the relative importance of the two bending energies.

In total, we have now identified the three parameters that are needed to describe vesicle shapes: 1) the ratio of the elastic moduli α, 2) the effective spontaneous curvature $\bar{m}_0$, and 3) the reduced volume v. The ratio of the elastic moduli is given by the lipid system studied and is essentially fixed in each set of experiments. We are thus left with the geometrical quantity v and the effective spontaneous curvature $\bar{m}_0$. Observed shapes can therefore be placed in a two-dimensional phase diagram (see Fig. 7). All the shapes shown, except the dashed ones, which are discussed below, are drawn to scale and globally minimize the elastic energy of the membrane. They all have the same area and differ only in reduced volume v, which is depicted by the horizontal axes. The vertical axis measures the effective spontaneous curvature $\bar{m}_0$. Since we are interested in differential area effects, we have set the intrinsic spontaneous curvature c_0 to zero, i.e., $\bar{m}_0 = 4\ \pi\Delta a_0$. (A nonzero c_0 produces an overall shift, and changes in Δa_0 are relative in this sense.) Shapes are placed according to their approximate position in the phase diagram. The important fact to notice is that all outwardly curved shapes are in the upper part of the diagram at large Δa_0, whereas all inwardly curved shapes are in the lower part at small Δa_0 irrespective of their reduced volume. All shapes are rotational symmetric bodies with their symmetry axis along the vertical, except the dashed ones, which have no rotational symmetry. The evolvement of vesicle contours at fixed reduced volume v with an increasing number of molecules on the outer monolayer as measured by Δa_0 can be followed as the latter parameter gets larger. Note the apparent increase in projected area at fixed real membrane area.

Having gone through this formal exposition of the theory of vesicle shapes we are now in a position to discuss our experimental findings in appropriate terms. We will identify the various experimental determinants and proceed then to a classification of the observed shapes and shape transitions.

Experimental shape determinants

The first factor determining shape that comes to mind is the preparation process of the vesicle. The shearing involved in extruding an MLV through a 100-nm filter may influence the relative areas between the inner and outer monolayers by affecting the curvature, and hence the relative outer and inner monolayer areas of the membrane fragment just before it breaks off and re-anneals to form the LUV. The degree of stretching or compression of the monolayers of the fragment will also play a role, because the monolayer areas will tend to relax back to their unstressed state when the vesicle reseals. These factors are influenced by lipid composition, and the temperature, speed, pressure and filter pore size used in the extrusion process. They generally lead to a distribution in Δa_0.

Other environmental factors are also important. There is much literature (Winterhalter and Helfrich, 1988; Mitchell and Ninham, 1989) on the electrostatic contributions to the spontaneous curvature, which is determined by the charge on the two sides of the membrane and the electrolyte concentrations of the inner and outer solutions. So, in addition to molecular shape factors and transbilayer lipid asymmetry, the adjacent solutions play a major role. More generally, not only will the spontaneous curvature c_0 be influenced by the vesicle environment, but also the difference in monolayer areas Δa_0 is affected via asymmetric changes in the molecular areas (Kozlov et al., 1992).

All these effects can be subsumed in the effective spontaneous curvature $\bar{m}_0$. From the above discussion it becomes clear that the initial conditions for a vesicle ensemble have to be determined and well characterized before controlled changes in the shape-determining factors are made. The main objective of this work is to demonstrate the role of the monolayer differential area Δa_0. We did not attempt to vary other shape factors. On the contrary, care has been taken to ensure that shapes are compared with reference only to a common starting point. In all experiments, except when lyso-PC was added, the internal and external buffers were not changed when shape changes were induced by lipid translocation. In particular, the reduced volume of the vesicles was not affected by osmotically induced water flow. The distribution of reduced volume was determined by

the extrusion process and incubation buffers before the experiment.

Another important variable is the temperature of the samples just before vitrification. All samples were quenched from room temperature. This is crucial as changes in temperature affect the membrane area and therefore the reduced volume V (see Eq. 3). Likewise, as can be seen from Eq. 4, the effective spontaneous curvature $\bar{m}_0$ has a temperature dependence via the membrane area. In total, the temperature dependence of the point $(\bar{m}_0, v)$ defines a temperature trajectory in the phase diagram. Along that line the shape parameters change, and this is reflected in the vesicle shape. Indeed, this is one way in which shape transitions are induced in giant vesicles (Berndl et al., 1990; Käs and Sackmann, 1991). Heating to 60°C will thus have affected the shape in addition to the translocation of lipids due to the applied pH gradient. The important point here is that after cooling, these temperature effects will have been reversed and only the change in Δa_0 resulting from flip-flop of PG will contribute to the observed changes in vesicle shape.

The equilibrium area difference Δa_0 is easily related to the actual difference in the number of molecules ΔN in the two monolayers; thus, we have

$$\frac{\Delta N}{N} \simeq \frac{\Delta A_0}{A} = \frac{8\pi D R_A \Delta a_0}{4\pi R_A^2} = \frac{2D}{R_A}\Delta a_0. \tag{5}$$

One observes that the percentage of lipids that have to be transferred from one monolayer to the other to induce a significant shape change depends on the size of the vesicle. For giant vesicles the scaling factor $2\,D/R_A$ is on the order of 10^{-3}, and therefore only a very small percentage in the range of 0.1% or less is needed. The dramatic magnification effect of this factor has already been noted in the literature (Berndl et al., 1990; Farge and Devaux, 1993). Vesicles used in the present study have a diameter of ~100 nm; taking a bilayer thickness of 5 nm we find

$$\Delta a_0 \simeq 5\,\frac{\Delta N}{N}. \tag{6}$$

As shown in Fig. 1, almost complete translocation of DOPG from the inner to the outer monolayer, and vice versa, could be achieved. Given the ratio of (PC:Chol):PG = 9:1 employed, the shift induced in Δa_0 was therefore about 1 in either direction:

$$\Delta a_0^{\pm} \simeq 5\,\frac{\Delta N \pm 0.2N}{N} \simeq \Delta a_0 \pm 1 \tag{7}$$

This is approximately what is needed to induce the observed shape transitions at the range of reduced volume (0.2,0.98) found in our system (Miao et al., 1994). The agreement is considerably better than an order of magnitude by comparison. For an in-depth analysis the contours of the vesicles would have to be digitized and their shapes characterized in detail by a modal expansion. Such a procedure goes beyond the scope of this paper but is entirely possible and has been carried out for giant vesicles (Döbereiner, 1995). In fact, a careful analysis of the shape allows a measurement of the effective spontaneous curvature of the membrane. Instead of performing such a detailed analysis we restrict the discussion to the observed symmetry classes.

Before we proceed further, a comment on a recent paper is warranted (Farge and Devaux, 1993). It is shown theoretically in this work that shape changes in LUVs with quasi-spherical geometries are impeded by the accumulation of monolayer stress caused by lipid redistribution (compare Eq. 2). Taking a slightly different viewpoint we will obtain this result for nearly spherical vesicles. But we also argue that for flaccid vesicles shape changes can indeed be induced, as our experimental results clearly demonstrate.

The expression for the bending energy recalled in Eq. 2 can be derived from a simplified microscopic model of stress distribution in the bilayer (Miao et al., 1994; Svetina et al., 1985) and is actually the first term in an expansion of the elastic energy in powers of D/R_A. Retaining only the first term is essentially equivalent to the idealization of the membrane as a two-dimensional sheet. At this level the theory is entirely scale-invariant and the shapes and shape transitions of the vesicles are independent of their size. The next terms are smaller by a factor D/R_A, which makes it an excellent approximation to neglect any higher order terms in giant vesicle. Even in LUVs one still captures 90% of the energetics by restricting the modeling to the first term. One is thus confident that conclusions drawn from Eq. 3 hold true at least semiquantitatively. In particular, the topology of the phase diagram and the approximate location of phase boundaries will be the same.

For the case of the budding transition, where a small vesicle is expelled from the parent vesicle connected by a narrow neck, the location of the phase boundary between the prolate unbudded shape and the two-sphere configuration has been worked out in detail (Miao et al., 1994). In the asymptotic regime for large reduced volume, one finds for the difference in the number of molecules between the two shapes

$$\left.\frac{\Delta N}{N}\right|_{\text{budded}} - \left.\frac{\Delta N}{N}\right|_{\text{unbudded}} \sim \frac{D}{R_A}\frac{1}{\alpha}\left(\frac{R_1}{R_2} + 1\right), \tag{8}$$

where R_1 and R_2 are the radii of the large and small sphere, respectively, and R_A is the area-equivalent radius of the vesicle. In the spherical limit ($v \to 1$) we have $R_1 \to R_A$, and it is apparent that one has to pump more and more lipid to the outside monolayer the smaller the radius R_2 of the bud gets; i.e., it becomes harder and harder to induce the transition. This rather pathological result is actually correct in certain limits and reflects the fact that for a quasi-spherical vesicle there is hardly any area available for the bud (recall that the sphere is the geometrical object which has the smallest area for a given volume). However, as soon as there is more area available to change the shape at a reduced volume v sufficiently less than 1, the vesicle will simply adjust its integrated mean curvature to accommodate an

increase or decrease in the equilibrium differential monolayer area. Inspection of the phase diagram shows that for reduced volume $v \leq 0.97$ the required change in $\bar{m}_0$ is of the order of unity or less, and shape transitions are readily achievable as both indicated by Eq. 4 and experimental observations. These arguments are not restricted to the budding transition but hold true for any shape change.

We continue now with the discussion of the observed shape classes in our system. Let us compare the shapes and shape transitions seen in Figs. 3 and 5 to the phase diagram shown in Fig. 7. It is evident that the equilibrium differential area Δa_0 is most suitable to describe the ensembles at hand. Vesicles with an excess of molecules on the outside monolayer correspond to shapes in the upper half of the diagram, whereas vesicles with an increased number of molecules on the inside monolayer have a counterpart in the lower half. In fact, the contours of most of the vesicle shapes seen in Figs. 3 and 5 can be found in Fig. 7. The theoretical shapes are rotational symmetric bodies with their axes of symmetry within the projection plane and this is presumably also true for the experimental vesicle shapes, as most clearly seen in Fig. 5. The apparent breaking of this symmetry by the bending of the long tubes in Fig. 3 *B* reflects the freezing-in of non-axisymmetric thermal fluctuations of the vesicles around their rotational symmetric mean shape. The shape parameters v and Δa_0 are multivalued even within one ensemble, and their distribution leads to the variety of shapes within the two main classes. Most notable are the beaded tubes. These shapes can be classified by the number of beads. Simple dumbbells and higher multiplets are clearly visible. The very long tubes evolve continuously from simple dumbbells when their volume-to-area ratio is reduced, the beading amplitude becoming smaller and smaller in the process. Some intermediate representatives of this path in the phase diagram seem to be present in the micrographs.

Another interesting shape with a threefold symmetry is seen in Fig. 4 *C*. This symmetry implies that the shape is not rotationally symmetric. And indeed, although vesicles tend to have axisymmetric shapes at large reduced volume, it is known that at lower reduced volume there exist stable non-axisymmetric shapes (Seifert et al., 1991; Heinrich et al., 1993). The triangular shape can be derived from the discocytic shape by breaking of the rotational symmetry. The contour is depicted as a dashed line in Fig. 7 with its axis coming out of the plane. Further decreasing the reduced volume would result in the starfish-like shape also shown in Fig. 7.

The bottle-shaped vesicles that are found in abundance in Figs. 2 and 4 have so far not been identified in the phase diagram. This may be due to the fact that in that region of the phase diagram containing non-axisymmetric shapes an extensive search has not yet been carried out. However as the appearance of further appendages and fragments at higher PG asymmetry suggest (Fig. 2 *C*), we might have oversimplified the discussion so far. Any effects that result from the exact composition of the membrane have been neglected. The theory presented implicitly assumed a laterally homogeneous membrane.

The role of lipid composition

The different lipids employed in this study mix well, and there is no thermodynamic phase separation in our systems that would lead to membrane domains with unequal elastic parameters. However, the reverse effect is also possible; lipids with different elastic parameters can actually drive phase segregation in a system that is in a single thermodynamic phase (Seifert, 1993). For giant vesicles the effect is negligible, given that the entropy of mixing tends to counteract any buildup of lateral inhomogeneity. In small vesicles the situation is quite different, because the bending energy is scale-invariant and becomes more and more important the smaller the vesicles get. The lipid composition couples to the spontaneous curvature of the membrane, and therefore different lipid species will accumulate in regions of low or high curvature. The tubular structures formed when transbilayer DOPG asymmetry is induced in DOPC:DOPG:Chol (6:1:3) LUVs are smoother and more stable than in DOPC:DOPG (9:1) LUVs (Figs. 2 and 3). The presence of cholesterol might stabilize these structures because of molecular shape differences between cholesterol and DOPC and DOPG (Cullis et al., 1990). The molecular shape of DOPC and DOPG is cylindrical, as the lateral diameters occupied by their headgroups and acyl chains are similar. Cholesterol, however, is wedge-shaped, as the lateral cross-sectional area occupied by its hydroxyl headgroup is smaller than the hydrophobic region of the lipid. Appropriate lateral and transversal redistribution of cholesterol would therefore sterically stabilize regions of high curvature. Indeed, there is strong evidence that cholesterol is able to undergo relatively rapid transbilayer movement (Schroeder et al., 1991). The fact that similar morphological changes are observed in the presence of cholesterol as in the absence of cholesterol suggests that it is thermodynamically much more favorable for the vesicle to undergo dramatic shape changes in response to differences between the areas of inner and outer monolayers than to induce excessive compensatory transbilayer redistributions of lipid. In general, there will be a balance between lateral curvature-induced segregation and transversal migration of cholesterol such as to minimize the free energy of the system.

Implications for cellular transport

The observations of shape changes on cellular length scales driven by transbilayer lipid transport supports the possibility that the bending elasticity of bilayers could play an important role in intracellular membrane transport processes, as has been suggested in the literature (Sackmann et al., 1986; Oster et al., 1989; Lipowsky, 1991, 1992; Devaux, 1991; Döbereiner et al., 1993)

The hypothesis is that biochemical regulation adjusts the elastic parameters of the membrane, but that the actual morphological changes are governed by the physics of the elastic membrane. Such a description should also include the protein coats (Oster et al., 1989; Lipowsky, 1992; Döbereiner et al., 1993; Jin and Nossal, 1993). A specific example of such an interplay between shape mechanics and membrane biochemistry are protein pumps that transport lipid from one monolayer to the other, the existence of which has been proposed (Devaux, 1991).

The results presented here are clearly consistent with these ideas. We have demonstrated that shape changes on the cellular length scale can be controlled by regulating the difference in monolayer areas. The beaded structures seen in Figs. 3 *B*, 5 *B*, and 7 are reminiscent of endocytosis from the plasma membrane or budding from the Golgi stacks (Pfeffer and Rothman, 1987). The tubular projections formed when excess lipid is present in the outer monolayer of the membrane (see Figs. 2 and 3) resemble the "tubulovesicular" structures that have been observed between the cisternae of both the endoplasmic reticulum and the trans-Golgi network (Cooper et al., 1990; Lee et al., 1988; Dabora and Sheetz, 1988; Lippincott-Schwartz et al., 1990).

According to the above hypothesis, the precise molecular mechanism of differential area control is not directly coupled to morphological changes. In fact, every biochemical process that controls area would be effective. New area could be created by phospholipid biogenesis, which occurs predominantly on the cytoplasmic face of the endoplasmic reticulum (Bishop and Bell, 1988), or existing area could be relocated by transbilayer lipid pumps transporting lumenal lipid to the cytoplasmic monolayer. In any case, a necessary requirement for the control mechanisms is that they produce unidirectional flow of area between cellular compartments.

Another interesting observation to note is the appearance of vesicle fragments as shown in Fig. 2 *C*. Such structures might have fissioned off from larger vesicles. Such a process has recently been reported in giant as well as small vesicles made from lipid mixtures (Madden et al., 1988; Döbereiner et al., 1993). Indeed, it was found that mixed lipid composition is a major factor, since in monolipid vesicles buds expelled from the parent vesicle usually stay connected by a narrow neck. We have thus identified in our system two of the basic morphological characteristics of cellular transport: formation and separation of vesicular compartments.

SUMMARY

The results presented here establish LUV systems as useful models for examining the morphological consequences of differences between the inner and outer monolayer surface areas and more generally other environmental factors. The morphological properties of extruded LUV systems are interpreted within the context of bending energies of lipid membranes. Further, the observations made here provide support for the proposal that transbilayer lipid transport processes could play an important role in the intracellular trafficking of membranes.

We thank E. Evans, L. Miao, M. Nikolić, U. Seifert, and M. Wortis for helpful discussions.

This work was supported by the Medical Research Council of Canada and the International Council for Canadian Studies.

REFERENCES

Berndl, K., J. Käs, R. Lipowsky, E. Sackmann, and U. Seifert. 1990. Shape transformations of giant vesicles: extreme sensitivity to bilayer asymmetry. *Europhys. Lett.* 13:659–664.

Bishop, W. R., and R. M. Bell. 1988. Assembly of phospholipid into cellular membranes: biosynthesis, transmembrane movement and intracellular translocation. *Annu. Rev. Cell Biol.* 4:579–610.

Canham, P. B. 1970. The minimum energy of bending as a possible explanation of the biconcave shape of the humam red blood cell. *J. Theor. Biol.* 26:61–81.

Cooper, M. S., Cornell-Bell, A. Chernjavsky, J. W. Dani, and S. J. Smith. 1990. Tubulovesicular processes emerge from trans-Golgi cisternae, extended along microtubules, and interlink adjacent trans-Golgi elements into a reticulum. *Cell.* 61:135–145.

Cullis, P. R., C. P. Tilcock, and M. J. Hope. 1990. Lipid polymorphism. *In* Membrane Fusion. J. Wilschut and D. Hoekstra, editors. Marcel Dekker, New York. 35–64.

Dabora, S. L., and M. P. Sheetz. 1988. The microtubule-dependent formation of a tubulovesicular network with characteristics of the ER from cultured cell extracts. *Cell.* 54:27–35.

Deuling, H. J., and W. Helfrich. 1976. The curvature elasticity of fluid membranes: a catalogue of vesicle shapes. *J. Phys. (Paris).* 37: 1335–1345.

Devaux, P. F. 1991. Static and dynamic lipid asymmetry in cell membranes. *Biochemistry.* 30:1163–1173.

Döbereiner, H.-G. 1995. The budding transition of phospholipid vesicles: a quantitative study via phase contrast microscopy. Ph. D. Thesis, Simon Fraser University.

Döbereiner, H.-G., J. Käs, D. Noppl, I. Sprenger, and E. Sackmann. 1993. Budding and fission of vesicles. *Biophys. J.* 65:1396–1403.

Eastman, S. J., M. J. Hope, and P. R. Cullis. 1991. Transbilayer transport pf phosphatic acid in response to transmembrane pH gradients. *Biochemistry.* 30:1740–1745.

Evans, E. A. 1974. Bending resistance and chemically induced moments in membrane bilayers. *Biophys. J.* 14:923–931.

Evans, E. A. 1980. Minimum energy analysis of membrane deformation applied to pipet aspiration and surface adhesion of red blood cells. *Biophys. J.* 30:265–284.

Farge, E., and P. F. Devaux, 1992. Shape changes of giant liposomes induced by an asymmetric transmembrane distribution of phospholipids. *Biophys. J.* 61:347–357.

Farge, E., and P. F. Devaux. 1993. Size-dependent response of liposomes to phospholipid transmembrane redistribution: from shape change to induced tension. *J. Phys. Chem.* 97:2958–2961.

Fiske, C. H., and Y. Subbarow. 1925. The colorimetric determination of phosphorus. *J. Biol. Chem.* 66:375–400.

Gebhardt, C., H. Gruler, and E. Sackmann. 1977. On domain structure and local curvature in lipid bilayers and biological membranes. *Z. Naturforsch.* 32c:581–596.

Heinrich, V., S. Svetina, and B. Žekš. 1993. Nonaxisymmetric vesicle shapes in a generalized bilayer-couple model and the transition between oblate and prolate axisymmetric shapes. *Phys. Rev. E.* 48:3112–3123.

Helfrich, W. 1973. Elastic properties of lipid bilayers: theory and possible experiments. *Z. Naturforsch.* 28c:693–703.

Helfrich, W. 1974. Blocked lipid exchanges in bilayers and its possible influence on the shape of vesicles. *Z. Naturforsch.* 29c:510–515.

Hope, M. J., M. B. Bally, G. Webb, and P. R. Cullis. 1985. Production of large unilamellar vesicles by rapid extrusion procedure. Characterization of size distribution, trapped volume and ability to maintain a membrane potential. *Biochim. Biophys. Acta.* 812:55–65.

Hope, M. J., T. E. Redelmeier, K. F. Wong, W. Rodriguez, and P. R. Cullis. 1989. Phospholipid asymmetry in large unilamellar vesicles induced by transmembrane pH gradients. *Biochemistry* 28:4181–4187.

Jin, A. J., and R. Nossal. 1993. Topological mechanism involved in the formation of clathrin-coated vesicles. *Biophys. J.* 65:1523–1537.

Jülicher, F., and R. Lipowsky. 1993. Domain-induced budding of vesicles. *Phys. Rev. Lett.* 70:2964–2967.

Käs, J., and E. Sackmann. 1991. Shape transitions and shape stability of giant phospholipid vesicles in pure water induced by area-to-volume changes. *Biophys. J.* 60:825–844.

Kozlov, M. M., M. Winterhalter, and D. Lerche. 1992. Elastic properties of strongly curved monolayers. Effect of electric surface charges. *J. Phys. II France.* 2:175–185.

Lee, C., and L. B. Chen. 1988. Dynamic behavior of endoplasmic reticulum in living cells. *Cell.* 54:37–46.

Lipowsky, R. 1991. The conformation of membranes. *Nature.* 349: 475–481.

Lipowsky, R. 1992. Budding of membranes induced by intramembrane domains. *J. Phys. II.* 2:1825–1840.

Lippincott-Schwartz, J., J. G. Donaldson, A. Schweizer, E. G. Berger, H.-P. Hauri, L. C. Yuan, and R. D. Klausner. 1990. Microtubule-dependent retrogade transport of proteins into the ER in the presence of brefeldin A suggest an ER recycling pathway. *Cell.* 60:821–836.

Madden, T. D., C. P. S. Tilcock, K. Wong, and P. R. Cullis. 1988. Spontaneous vesiculation of large multilamellar vesicles composed of saturated phosphatidylcholine and phosphatidylglycerol mixtures. *Biochemistry.* 27:8724–8730.

Markin, V. S. 1981. Lateral organization of membranes and cell shape. *Biophys. J.* 36:1–19.

Marsh, D. 1990. Handbook of Lipid Bilayers. CRC Press, Boca Raton.

Mayer, L. D., M. J. Hope, P. R. Cullis, and A. S. Janoff. 1985. Solute distribution and trapping efficiencies observed in freeze-thawed multilamellar vesicles. *Biochim. Biophys. Acta.* 817:193–196.

Meunier, J., D. Langevin, and N. Boccara, editors. 1987. Physics of Amphiphilic Layers. *Springer Proc. Phys.* 21.

Miao, L., B. Fourcade, M. Rao, M. Wortis, and R. K. P. Zia. 1991. Equilibrium budding and vesiculation in the curvature model of fluid lipid vesicles. *Phys. Rev. A.* 43:6843–6856.

Miao L., U. Seifert, M. Wortis, and H.-G. Döbereiner. 1994. Budding transitions of fluid-bilayer vesicles: the effect of area-difference elasticity. *Phys. Rev. E.* 49:5389–5407.

Mitchell, D. J., and B. W. Ninham. 1989. Curvature elasticity of charged membranes. *Langmuir.* 5:1121–1123.

Oster, G. F., L. Y. Cheng, H.-P. H. Moore, and A. S. Perelson. 1989. Vesicle formation in the Golgi apparatus. *J. Theor. Biol.* 141:463–504.

Pfeffer, S. R., and J. E. Rothman. 1987. Biosynthetic protein transport and sorting by the endoplasmatic reticulum and Golgi. *Annu. Rev. Biochem.* 56:829–852.

Redelmeier, T. E., M. J. Hope, and P. R. Cullis. 1990. On the mechanism of transbilayer transport of phosphatidylglycerol in response to transmembrane pH gradients. *Biochemistry.* 29:3046–3053.

Sackmann, E., H.-P. Duwe, and H. Engelhardt. 1986. Membrane bending elasticity and its role for shape fluctuations and shape transformations of cells and vesicles. *Faraday Discuss. Chem. Soc.* 81:281–290.

Schroeder, F., J. R. Jefferson, A. B. Kier, J. Knittel, T. J. Scallen, W. G Wood, and I. Hapala. 1991. Membrane cholesterol dynamics: cholesterol domains and kinetic pools. *Proc. Soc. Exp. Biol. Med.* 196: 235–252.

Seifert, U., K. Berndl, and R. Lipowsky. 1991. Shape transformations of vesicles: phase diagrams for spontaneous-curvature and bilayer-coupling models. *Phys. Rev. A.* 44:1182–1202.

Seifert, U., L. Miao, H.-G. Döbereiner, and M. Wortis. 1992. The structure and conformation of amphiphilic membranes. R. Lipowsky, D. Richter, and K. Kremer, editors. Springer-Verlag Berlin. *Springer Proc. Phys.* 66:93–96.

Seifert, U. 1993. Curvature-induced lateral phase segregation in two-component vesicles. *Phys. Rev. Lett.* 70:1335–1338.

Sheetz, M. P, and S. J. Singer. 1974. Biological membranes as bilayer couples. A molecular mechanism of drug-erythrocyte interactions. *Proc. Natl. Acad. Sci. USA.* 71:4457–4461.

Svetina, S., M. Brumen, and B. Žekš. 1985. Lipid bilayer elasticity and the bilayer couple interpretation of red cell shape transformations and lysis. *Stud. Biophys.* 110:177–184.

Svetina, S., and B. Žekš. 1989. Membrane bending energy and shape determination of phospholipid vesicles and red blood cells. *Eur. Biophys. J.* 17:101–111.

Waugh, R., J. Song, S. Svetina, and B. Žekš. 1992. Local and nonlocal curvature elasticity in bilayer membranes by tether formation from lecithin vesicles. *Biophys. J.* 61:974–982.

Winterhalter, M., and W. Helfrich. 1988. Effect of surface charge on the curvature elasticity of membranes. *J. Phys. Chem.* 92:6865–6867.

Wortis, M., U. Seifert, K. Berndl, B. Fourcade, L Miao, M. Rao, and R. K. P. Zia. 1993. Curvature-controlled shapes of lipid-bilayer vesicles: budding vesiculation and other phase transitions. *In* Dynamical Phenomena at Interfaces, Surfaces and Membranes, Les Houches 1991. D. Beysens, N. Boccara, and G. Forgacs, editors. NovaScience, Commack. 221–235.